Sex-Specific Effect of Estrogen Sulfotransferase on Mouse Models of Type 2 Diabetes

Jie Gao,[1,2] Jinhan He,[1,2] Xiongjie Shi,[1,2] Maja Stefanovic-Racic,[3] Meishu Xu,[1,2] Robert Martin O'Doherty,[3] Adolfo Garcia-Ocana,[3] and Wen Xie[1,2,4]

Estrogen sulfotransferase (EST), the enzyme responsible for the sulfonation and inactivation of estrogens, plays an important role in estrogen homeostasis. In this study, we showed that induction of hepatic *Est* is a common feature of type 2 diabetes. Loss of *Est* in female mice improved metabolic function in *ob/ob*, dexamethasone-, and high-fat diet–induced mouse models of type 2 diabetes. The metabolic benefit of *Est* ablation included improved body composition, increased energy expenditure and insulin sensitivity, and decreased hepatic gluconeogenesis and lipogenesis. This metabolic benefit appeared to have resulted from decreased estrogen deprivation and increased estrogenic activity in the liver, whereas such benefit was abolished in ovariectomized mice. Interestingly, the effect of *Est* was sex-specific, as *Est* ablation in *ob/ob* males exacerbated the diabetic phenotype, which was accounted for by the decreased islet β-cell mass and failure of glucose-stimulated insulin secretion in vivo. The loss of β-cell mass in *ob/ob* males deficient in *Est* was associated with increased macrophage infiltration and inflammation in white adipose tissue. Our results revealed an essential role of EST in energy metabolism and the pathogenesis of type 2 diabetes. Inhibition of EST, at least in females, may represent a novel approach to manage type 2 diabetes. ***Diabetes*** **61:1543–1551, 2012**

Estrogens are implicated in various physiological functions besides reproduction. In recent years, the importance of estrogens in regulating energy and glucose homeostasis has gained increasing attention. Mice lacking aromatase, the enzyme that converts androgens to estrogens, develop obesity due to reduced physical activity and decreased lean body mass (1). The estrogen receptor α (ERα)–deficient mice also develop obesity with decreased energy expenditure (2). The mechanism by which estrogens stimulate energy expenditure is not fully understood. It is suggested that ERα signaling in the ventromedial nucleus of the hypothalamus plays an important role in regulating food intake, systemic insulin sensitivity, and energy expenditure in female mice (3). Estrogen deficiencies also lead to impaired insulin sensitivity in both aromatase knockout (1) and ERα knockout (4) mice but without a defined mechanism. Administration of estrogens, in contrast, improves insulin sensitivity in high-fat diet (HFD)–fed female mice (5) and *ob/ob* mice (6).

Estrogen homeostasis is tightly regulated through balanced biosynthesis and metabolism. Sulfation is a dominant estrogen transformation and inactivation pathway, because the sulfonated estrogens can no longer bind to ER (7). Estrogen sulfotransferase (EST, or SULT1E1) is a cytosolic enzyme catalyzing the transfer of sulfate from 3′-phosphoadenosine-5′-phosphosulfate to available hydroxyl groups of the estrogens. EST has been proposed to be the primary enzyme responsible for sulfonation and inactivation of estrogens at physiological concentrations. Consistent with the proposed function of EST in estrogen homeostasis, $Est^{-/-}$ males exhibit structural and functional lesions in their reproductive system, a phenotype resulting from chronic estrogen stimulation (8). In female $Est^{-/-}$ mice, the defect of estrogen sulfation causes estrogen excess, leading to placental thrombosis and spontaneous fetal loss (9).

Under normal conditions, the hepatic expression of *Est* in mice is rather low (10,11). An aberrant and marked induction of *Est* has been reported in the liver of the obese and diabetic C57BL/KsJ-*db/db* mice (12), whereas the expression of *Est* in testis is not affected in the same mice (13). Positive associations between diabetic phenotype and hepatic *Est* induction have also been reported in several other strains of female obese mice (14). However, whether and how Est plays a role in energy metabolism and pathogenesis of type 2 diabetes have not been reported. Mechanistically, the *Est* induction in obese and diabetic mice might have been mediated by the glucocorticoids and glucocorticoid receptor (GR). The *ob/ob* phenotype is known to be associated with an increased glucocorticoid level (15). Chronic treatment of wild-type (WT) mice with dexamethasone (DEX), a synthetic glucocorticoid, is sufficient to induce hyperglycemia and hyperinsulinemia (16), which is associated with the induction of Est because *Est* is a GR target gene (11).

In this report, we show that loss of *Est* has a sex-specific effect on mouse models of type 2 diabetes. Loss of *Est* improves and exacerbates metabolic functions in female and male *ob/ob* mice, respectively. Est may achieve its effect on energy metabolism by regulating body composition, energy expenditure, insulin sensitivity, and β-cell mass.

RESEARCH DESIGN AND METHODS

Animals. *ob/ob* mice lacking *Est* (*obe*) were generated by crossing heterozygous B6.V-Lepob/J mice from The Jackson Laboratory with $Est^{-/-}$ mice in a C57BL/6J background (8) until both alleles reach homozygosity. Food intake and weights were determined weekly. All studies were performed on age-matched mice. HFD (catalog number S3282) was purchased from Bio-serv (Frenchtown, NJ). Body composition was analyzed in live animals using EchoMRI-100 from Echo Medical Systems (Houston, TX). The use of mice in this study has complied with all relevant federal guidelines and institutional policies.

From the [1]Center for Pharmacogenetics, University of Pittsburgh, Pittsburgh, Pennsylvania; the [2]Department of Pharmaceutical Sciences, University of Pittsburgh, Pittsburgh, Pennsylvania; the [3]Department of Medicine, Division of Endocrinology and Metabolism, University of Pittsburgh, Pittsburgh, Pennsylvania; and the [4]Department of Pharmacology and Chemical Biology, University of Pittsburgh, Pittsburgh, Pennsylvania.
Corresponding author: Wen Xie, wex6@pitt.edu.
Received 17 August 2011 and accepted 2 February 2012.
DOI: 10.2337/db11-1152
This article contains Supplementary Data online at http://diabetes.diabetesjournals.org/lookup/suppl/doi:10.2337/db11-1152/-/DC1.

See accompanying commentary, p. 1353.

Indirect calorimetry. This was performed using an Oxymax Indirect Calorimetry System from Columbus Instruments (Columbus, OH). Mice were individually housed in the chamber with a 12-h light/12-h dark cycle in an ambient temperature of 22–24°C. Metabolic rate, respiratory quotient (ratio of CO_2 produced to O_2 consumed), and physical activity were evaluated over a 48-h period. Mice were acclimatized overnight before data collection.

Euglycemic-hyperinsulinemic clamp. The clamp experiments were performed as described by others (17). Briefly, right jugular veins of 7- to 8-week-old *ob/ob* or *obe* mice were catheterized 4 days before the experiment, and mice were fasted 16 h before euglycemic clamps. On the day of the clamp experiment, the mouse was placed in a rat-size restrainer with its tail tape-tethered at one end at least 2 h in order for the mouse to acclimatize to the restrained state. D-[3-^{3}H] glucose (0.05 μCi/min) was infused for 2 h, and blood samples were collected from the tail vein to assess the basal rate of whole-body glucose turnover. Following the basal period, the mouse was infused with a primed (300 mU/kg body weight) and continuous infusion (12.5 mU/kg/min) of human insulin (Novolin) from Novo Nordisk (Princeton, NJ). Blood glucose levels were measured in 10-min intervals, and a variable 20% glucose was infused to maintain glucose at 120–150 mg/dL. Blood samples (20 μL) at 100, 110, and 120 min were collected for the measurement of plasma [3-^{3}H] glucose, and insulin levels were measured in the final blood sample.

Glucose tolerance, insulin tolerance, and glucose-stimulated insulin secretion tests. For glucose tolerance tests (GTT), mice were fasted for 16 h before receiving an intraperitoneal injection of D-glucose at 1 g/kg body weight (for *ob/ob* mice) or 2 g/kg body weight (for other genotypes). Blood glucose concentrations were measured with a glucometer. For insulin tolerance tests

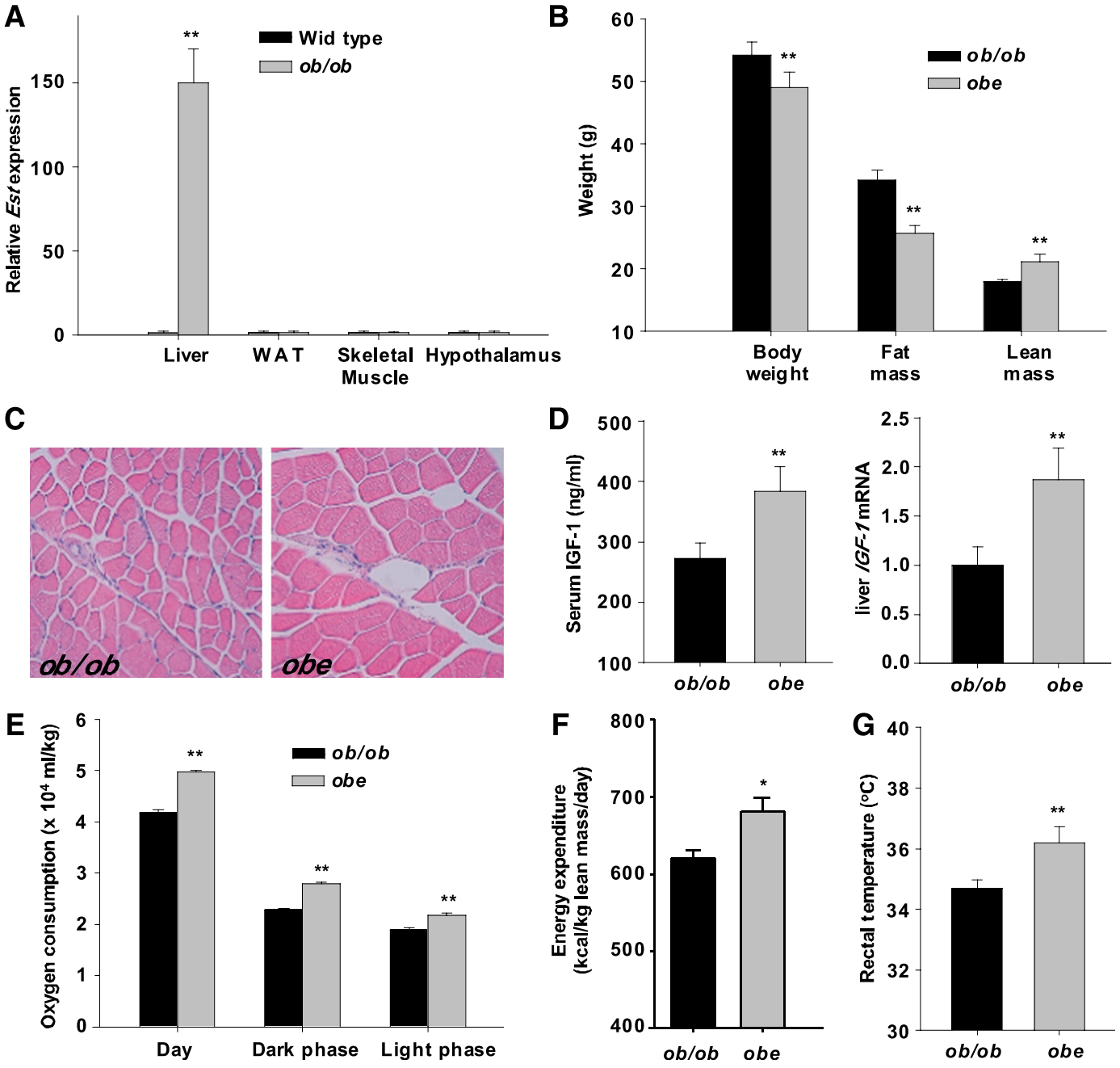

FIG. 1. Loss of *Est* inhibited adiposity and improved metabolic functions in *ob/ob* female mice. *A*: Expression of *Est* in female WT C57BL/6J and *ob/ob* mice as determined by real-time PCR analysis. *B*: Body composition analysis of 12-week-old female mice. *C*: H-E staining of gastrocnemius muscle. *D*: Serum IGF-1 level and hepatic *IGF-1* mRNA expression. Oxygen consumption (*E*) and energy expenditure (*F*) were measured by comprehensive laboratory animal monitoring system. *G*: Measurement of rectal temperature. $N \geq 4$ for each group. *$P < 0.05$; **$P < 0.01$, *ob/ob* versus *obe*. (A high-quality color representation of this figure is available in the online issue.)

(ITT), mice were fasted for 4 h before receiving an intraperitoneal injection of insulin at 0.5 or 1.5 units/kg body weight. For glucose-stimulated insulin secretion (GSIS) tests, an additional 20 μL blood was collected from the 30-, 60-, and 120-min time points during GTT for the measurement of plasma insulin levels. Mouse islets were isolated, and in vitro GSIS was performed as previously described (18).

Histochemistry and immunofluorescence microscopy. Tissues were fixed in 4% formaldehyde, embedded in paraffin, sectioned at 5 μm, and stained with hematoxylin-eosin (H-E) (19). For immunofluorescence, tissue sections were deparaffinized and rehydrated, followed by preincubated in blocking buffer (1× PBS, 5% normal donkey serum, and 0.3% Triton X-100) for 60 min. Tissue sections were then incubated with diluted primary antibody overnight at 4°C and fluorochrome-conjugated secondary antibody for 1 to 2 h at room temperature in dark the next day. Antibodies used include rabbit anti-human insulin (C27C9) monoclonal antibody (catalog number 3014; Cell Signaling Technology), goat anti-human glucagon (*N*-17) polyclonal antibody (catalog number sc-7780; Santa Cruz Biotechnology), and goat anti-mouse CD68 (M-20) polyclonal antibody (catalog number sc-7084; Santa Cruz Biotechnology). Histomorphometric analysis on insulin-stained pancreatic sections was performed using ImageJ from the National Institutes of Health (Bethesda, MD), and the percent of islet area per total pancreatic area was calculated (20). β-cell mass was determined by multiplying the percentage of islet area per pancreatic area by the pancreatic weight. Pancreatic β-cell proliferation and apoptosis were determined on insulin-stained pancreatic sections by Ki67 immunostaining (Ki67 antibody clone SP6; Neomarkers) and terminal deoxynucleotidyl transferase-mediated dUTP nick end-labeling (TUNEL) assay from Promega (Madison, WI), respectively (20).

Estrogen sulfotransferase enzymatic assay. This was performed as described previously (10). Briefly, 20 μg/mL total liver cytosolic protein extract was incubated with 1 μmol/L of estrone substrate and [^{35}S]phosphoadenosine phosphosulfate from PerkinElmer (Boston, MA) at 37°C for 30 min. The reaction was terminated by adding ethyl acetate, and the aqueous phase was then counted in a scintillation counter.

Serum chemistry. Serum levels of estradiol (E_2; catalog number DSL-4800), estrone (E_1; catalog number DSL-8700), estrone sulfate (E_1S; catalog number DSL-5400), thyroxine (T_4; catalog number DSL-3200), and triiodothyronine (T_3; catalog number DSL-3100) were measured using RIA assay kits from Diagnostic Systems Laboratories (Webster, TX). Serum levels of triglyceride (catalog number 2100-430; Stanbio), cholesterol (catalog number 1010-430; Stanbio), free fatty acids (catalog number 11383175001; Roche), insulin (catalog number 90080; Crystal Chem), and insulin-like growth factor-1 (IGF-1; catalog number MG100; R&D Systems) were measured by using commercial assay kits (Diagnostic Systems Laboratories) according to the manufacturer's instructions.

Quantitative RT-PCR. Total RNA was isolated using TRIzol reagent (Invitrogen). Reverse transcription was performed with random hexamer primers and Superscript RT III enzyme from Invitrogen. SYBR Green-based real-time PCR was performed with the ABI 7300 PCR System (Applied Biosystems). Data were normalized against cyclophillin.

Statistical analysis. Results are presented as the means ± SD. Statistical significance between groups was determined using an unpaired two-tailed Student *t* test, with *P* values of <0.05 considered significant.

RESULTS

***ob/ob* mice lacking *Est* had reduced adiposity and increased energy expenditure.** *Est* is known to have a low basal expression in the mouse liver (10,11). We showed that *ob/ob* mice had a dramatic and liver-specific induction of *Est* (Fig. 1*A*), consistent with the hepatic induction of the same gene in *db/db* mice (12,13). To determine the role of *Est* in the pathogenesis of type 2 diabetes in *ob/ob* mice, we crossbred $Est^{-/-}$ mice with heterozygous *ob/ob* mice to generate *ob/ob* mice lacking *Est* that were termed *obe* mice. Obe mice exhibited hyperphagia and early onset of obesity similar to *ob/ob* mice before 6 weeks of age. During adulthood, however, female, but not male, *obe* mice showed a modest but significant decrease in body weight compared with age-matched *ob/ob* females (Fig. 1*B*). Magnetic resonance imaging analysis revealed favorable body composition changes in *obe* mice that included decreased fat mass and increased lean mass (Fig. 1*B*), which was achieved without significant changes in food intake and physical activity (Supplementary Table 1). *ob/ob* mice were reported to be acyclic (21), suggesting that estrous cycle may not be an important factor in affecting food intake. Consistent with their increased lean mass, *obe* females showed increased skeletal muscle fiber bundle size (Fig. 1*C*) and increased gastrocnemius and soleus muscle weight (Supplementary Table 1), which was associated with an increased serum level of IGF-1 and increased *IGF-1* mRNA expression (Fig. 1*D*) in the liver, a tissue known to contribute up to 90% of circulating IGF-1 (22). A decreased IGF-1 level has been proposed to contribute to the decreased muscle mass in *ob/ob* mice (23). The improved body composition and unchanged food intake led to our hypothesis that *obe* females may have increased energy expenditure. Indeed, compared with their *ob/ob* counterparts, *obe* females had higher oxygen consumption (Fig. 1*E*), higher energy expenditure when normalized against the lean body mass (24) (Fig. 1*F*), and an ~1.5°C increase in resting rectal temperature (Fig. 1*G*). The metabolic benefit of loss of *Est* was not associated with altered serum levels of T_3 and T_4 (Table 1), although thyroid hormones have been reported as low-affinity EST substrates (25).

***Obe* female mice displayed improved insulin sensitivity and reduced hepatic steatosis.** In understanding the metabolic benefit of *Est* ablation, we found that *obe* females, but not males, showed reduced fasting hyperglycemia and improved performance in GTT and ITT (Fig. 2*A*). *Obe* females showed inhibition of hepatic gluconeogenesis as supported by their improved performance in a pyruvate tolerance test (data not shown). Using the hyperinsulinemic-euglycemic clamp test, we found that 8- to 9-week-old *obe* females showed significantly lower fasting glucose and insulin levels (Table 1) and a nearly threefold increase of glucose infusion rates during clamp period (Fig. 2*B*), suggesting a markedly improved insulin sensitivity. *Obe* females showed lower basal and clamp hepatic glucose production (HGP) (Fig. 2*C*), and significant suppression of HGP during clamp stage compared with *ob/ob* mice (Fig. 2*D*), which indicated improved hepatic insulin sensitivity. Consistent with reduced HGP, *obe* females showed a decreased hepatic expression of gluconeogenic genes, including *Pgc-1α*, *Pepck*, and *G6pase* (Fig. 2*E*). Female *obe* mice also exhibited relief of hepatic steatosis as shown by histology (Fig. 2*F*) and measurement of liver levels of triglycerides and cholesterol (Table 1). The expression of hepatic lipogenic and adipogenic genes *Srebp-1c*,

TABLE 1
Metabolic profile of *ob/ob* and *ob/ob-Est null* (*obe*) female mice

	ob/ob	*obe*
T_3 (nM)	1.43 ± 0.09	1.39 ± 0.19
T_4 (nM)	61.8 ± 7.2	50.8 ± 8.7
Fasting glucose (mg/dL)	132.7 ± 10.5	87.0 ± 6.4**
Fasting insulin (ng/mL)	5.73 ± 1.54	2.01 ± 0.43**
Liver triglyceride (mg/g tissue)	95.7 ± 5.9	32.0 ± 7.3**
Liver total cholesterol (mg/g tissue)	9.43 ± 1.64	1.64 ± 0.35**
Serum triglyceride (mg/dL)	184 ± 32	110 ± 19*
Serum total cholesterol (mg/dL)	129 ± 6	121 ± 11
Serum free fatty acid (mM)	0.96 ± 0.11	0.51 ± 0.15**
E_1 (pg/mL)	36.13 ± 2.40	44.37 ± 1.84*
E_1S (pg/mL)	644.2 ± 53.1	459.3 ± 98.5*
17β-E_2 (pg/mL)	9.09 ± 2.02	11.13 ± 2.14

*$P < 0.05$. **$P < 0.01$.

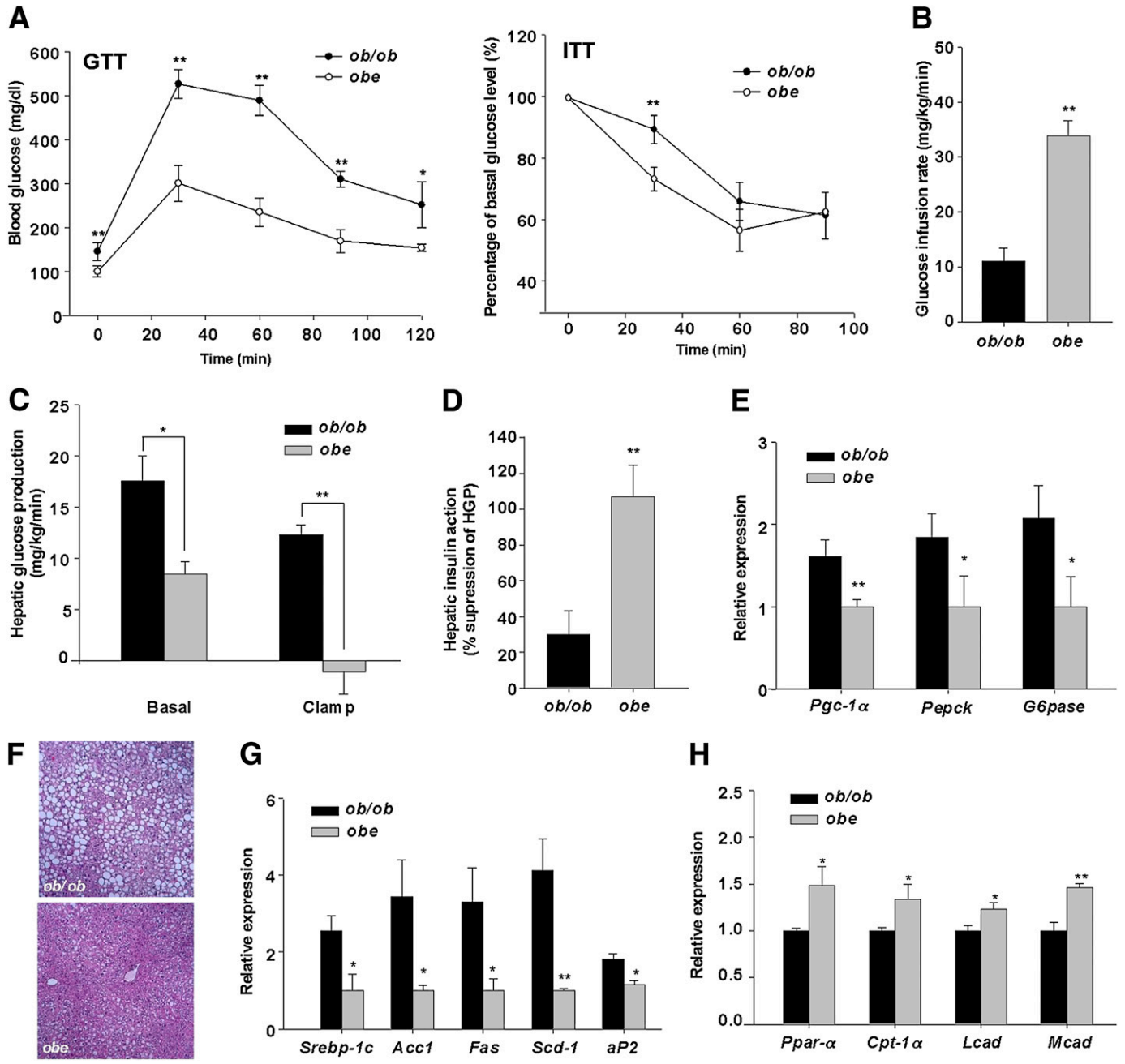

FIG. 2. ***Obe*** **female mice showed improved insulin sensitivity and reduced hepatic steatosis.** ***A*****: GTT and ITT on 9-week-old** ***ob/ob*** **and** ***obe*** **female mice. Glucose infusion rate (*** ***B*****), hepatic glucose production (*** ***C*****), and suppression of hepatic glucose production (*** ***D*****).** ***E*****: The expression of gluconeogenic genes in fasted mice as measured by real-time PCR analysis.** ***F*****: H-E staining of liver sections. The expression of hepatic lipogenic (*** ***G*****) and fatty acid oxidation (*** ***H*****) genes as measured by real-time PCR analysis.** $N \geq 4$ **for each group. *** $P < 0.05$**; **** $P < 0.01$**,** ***ob/ob*** **versus** ***obe*****. (A high-quality color representation of this figure is available in the online issue.)**

Acc1, *Fas*, *Scd-1*, and *aP2* was decreased (Fig. 2*H*), whereas the expression of fatty acid oxidative genes *Ppar-α*, *Cpt-1α*, *Lcad*, and *Mcad* was increased in *obe* females (Fig. 2*I*). The improved metabolic function of *obe* females was also manifested at the serum chemistry level, which included decreased circulating levels of triglycerides and free fatty acids (Table 1).

The metabolic benefit of *Est* deficiency was mediated through the estrogen pathway. Because the primary function of Est is to sulfonate and deactivate estrogens, and estrogens are known to improve the metabolic functions of *ob/ob* mice (6), we went on to determine whether the improved metabolic function in *obe* females was due to increased estrogenic activity in the liver. As shown in Fig. 3*A*, compared with *ob/ob* females, the hepatic expression of a panel of estrogen responsive genes was induced in *obe* females, which was consistent with the observation that the liver extracts of *obe* mice showed a substantially lower estrogen sulfotransferase activity (Fig. 3*B*). The estrogenic effect was liver-specific, because the expression of estrogen responsive genes was not affected in the skeletal muscle and white adipose tissue (WAT) (Supplementary Fig. 1*A*), despite modest increases in the serum levels of E_1 and its sulfated metabolite E_1S. The circulating level of E_2, the most potent estrogen, was not significantly affected in *obe* females (Table 1).

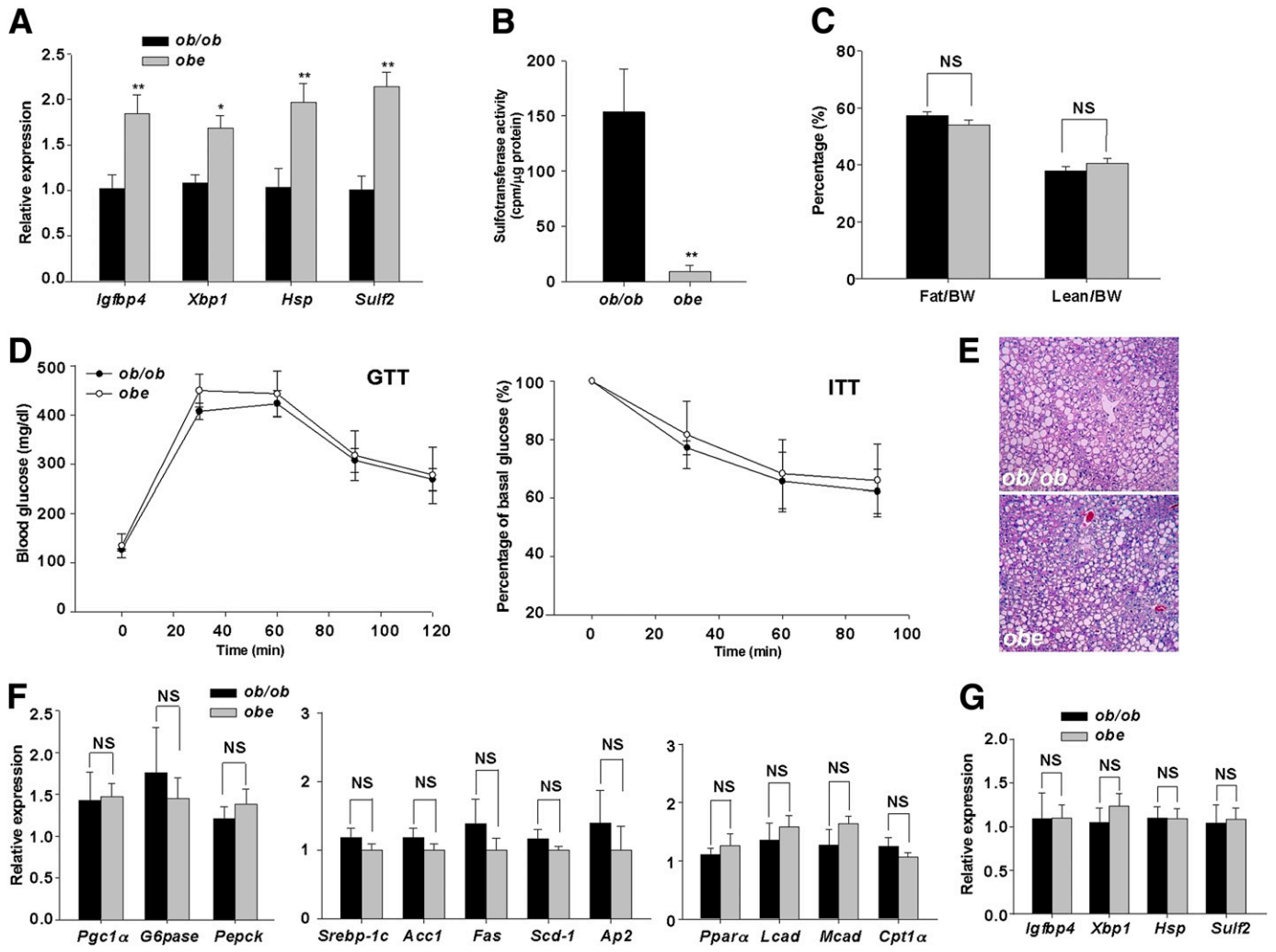

FIG. 3. The metabolic benefit of *Est* ablation was abolished in ovariectomized mice. Hepatic mRNA expression of estrogen-responsive genes (*A*) and measurement of estrogen sulfotransferase activity in the liver extracts (*B*) of intact *ob/ob* and *obe* mice. Body composition analysis (*C*), GTT and ITT (*D*), and H-E staining of liver section (*E*) in ovariectomized mice. The expression of gluconeogenic, lipogenic, and fatty acid oxidation genes (*F*) and estrogen-responsive genes (*G*) in ovariectomized mice as measured by real-time PCR analysis. $N \geq 4$ for each group. *$P < 0.05$; **$P < 0.01$; NS, statistically not significant, *ob/ob* versus *obe*. (A high-quality color representation of this figure is available in the online issue.)

To further evaluate the estrogen pathway, we performed ovariectomy on 5-week-old *ob/ob* and *obe* female mice and examined their metabolic functions 3 weeks after the surgery. Ovariectomy completely abolished the metabolic benefits of *obe* mice in body composition (Fig. 3*C*), IGF-1 protein and mRNA expression (Supplementary Fig. 1*B*), GTT and ITT performance (Fig. 3*D*), hepatic steatosis (Fig. 3*E*), and the expression of lipogenic, gluconeogenic, and fatty acid oxidative genes (Fig. 3*F*). The activation of hepatic estrogen-responsive genes in *obe* mice was also abolished upon ovariectomy (Fig. 3*G*).

Loss of *Est* inhibited DEX- and HFD-induced insulin intolerance in female mice. A chronic treatment of WT mice with DEX was sufficient to induce hyperglycemia with female mice showing a higher sensitivity (16). To determine whether DEX-induced hyperglycemia and insulin resistance was *Est*-dependent, we administrated DEX for 2 weeks to both WT and $Est^{-/-}$ mice. As expected, DEX treatment resulted in fasting hyperglycemia and glucose intolerance in WT females (Fig. 4*A*), which was associated with a marked induction of *Est* in the liver (Fig. 4*B*). In contrast, $Est^{-/-}$ females were resistant to DEX-induced hyperglycemia and showed improved GTT performance (Fig. 4*A*). Ovariectomy abolished the protective effect of *Est* ablation on DEX-induced insulin resistance (Supplementary Fig. 2). The loss of *Est* effect in the DEX model was female-specific, because $Est^{-/-}$ males remained sensitive to DEX-induced hyperglycemia (Fig. 4*C*). The antidiabetic effect of *Est* ablation was also observed in the HFD model. $Est^{-/-}$ females showed improved GTT and ITT performance upon 20 weeks of HFD feeding (Fig. 4*D*), which was associated with a hepatic induction of *Est* (Fig. 4*E*).

Loss of *Est* in *ob/ob* male mice aggravated diabetic phenotype, caused a loss of pancreatic β-cell mass, and increased WAT inflammation. Interestingly, the loss of *Est* effect on the *ob/ob* phenotype was sex-specific, because *obe* males had worsened diabetic phenotype compared with *ob/ob* males. As shown in Fig. 5*A*, *obe* males showed a higher fasting glucose level and worse GTT performance. The expression of estrogen-responsive genes was not affected in the liver of *obe* males (Fig. 5*B*), and castration failed to improve the metabolic function (Supplementary Fig. 3). In addition, *obe* males showed impaired GSIS, although the basal insulin level was

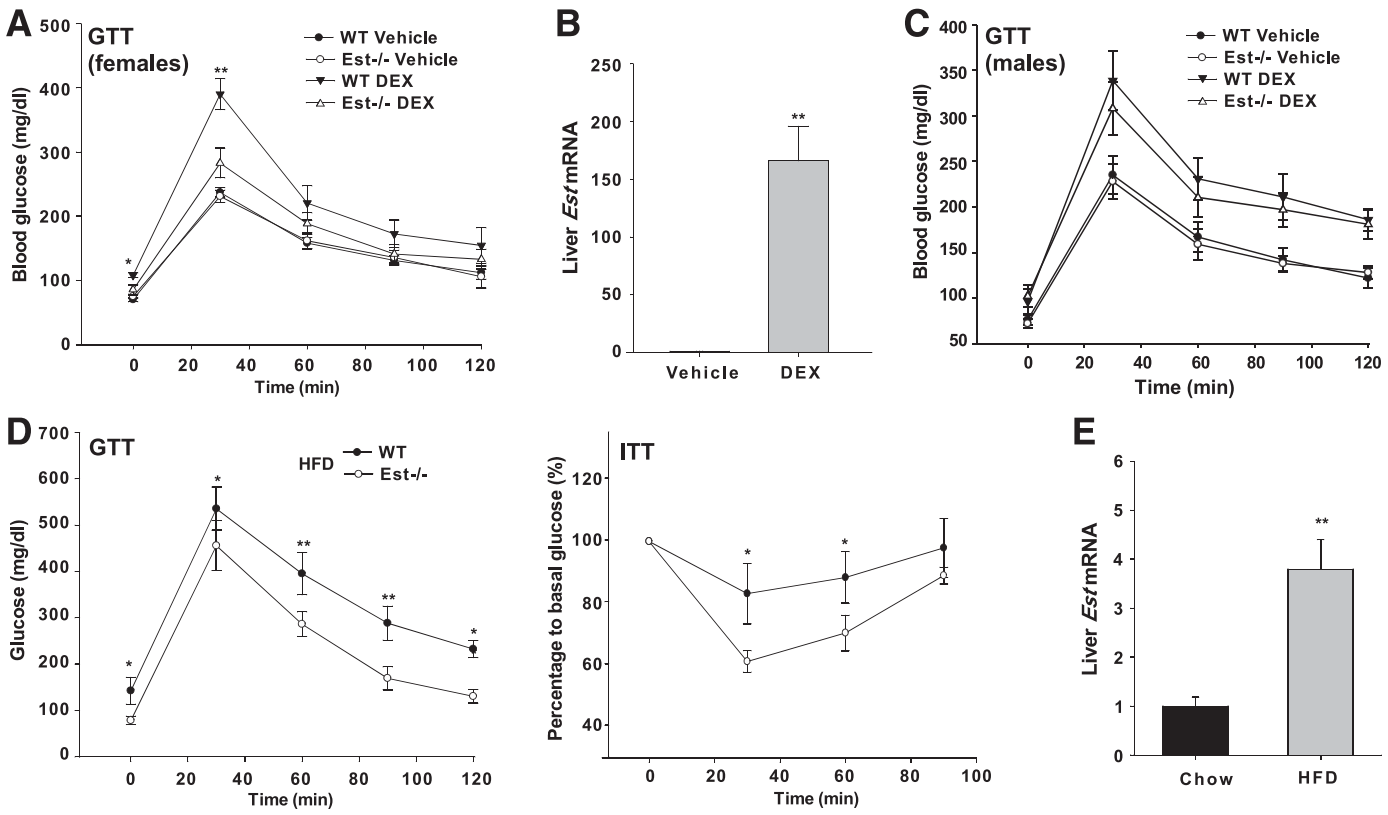

FIG. 4. Loss of *Est* inhibited DEX- and HFD-induced insulin intolerance. *A*: GTT in WT and *Est*$^{-/-}$ female mice treated with vehicle or DEX (daily i.p. injection at 1 mg/kg) for 2 weeks. *B*: Hepatic *Est* expression in DEX or vehicle-treated WT female C57BL/6J mice. *C*: GTT in WT and *Est*$^{-/-}$ male mice treated with vehicle or DEX. *D*: GTT and ITT in WT and *Est*$^{-/-}$ female mice fed with HFD for 20 weeks. *E*: Hepatic *Est* expression in WT female C57BL/6J mice fed with HFD for 20 weeks. *N* = 5 for each group. **P* < 0.05; ***P* < 0.01.

indistinguishable between *obe* and *ob/ob* males (Fig. 5*C*). Histological analysis of pancreatic sections showed dramatically reduced islet size, total islet area, and β-cell mass (Fig. 5*D* and Supplementary Fig. 4*A*) in *obe* males. This could suggest alterations in β-cell proliferation and/or death in *obe* mice. Indeed, when β-cell turnover was evaluated, we found that *obe* male mice displayed increased β-cell apoptosis but little change in β-cell proliferation compared with *ob/ob* male mice (Fig. 5*E*). Insulin and glucagon double staining revealed a normal distribution of endocrine cells in both *ob/ob* and *obe* males (Fig. 5*F*). The insulin-producing β-cells were evenly distributed, and the glucagon-producing α-cells were mainly located peripherally in the islets. There was a relative increase of α-cell in *obe* mice, possibly due to the decreased β-cell number. Islets of *obe* male mice were deformed with an increased infiltration of CD68-positive macrophages (Fig. 5*F*), which was suggestive of increased inflammation. Interestingly, islets isolated from *obe* males exhibited in vitro GSIS similar to those isolated from *ob/ob* males (Fig. 5*G*). These results suggested that the reduced β-cell mass might be responsible for the impaired insulin secretion upon glucose challenge. No expression of *Est* was detected in islets (data not shown), suggesting that the impaired insulin secretion was not due to the intrinsic loss of *Est* effect on β-cells. The loss of β-cell mass was not observed in *obe* females (Supplementary Fig. 4*B*).

In understanding the mechanism by which *Est* ablation exacerbated metabolic phenotype in *ob/ob* males, we found that *obe* males showed increased macrophage infiltration and inflammation in WAT as supported by increased density and size of the crownlike structures (Fig. 5*H*), as well as increased expression of several macrophage markers (*F4/80* and *CD68*) and inflammatory markers (*Mcp1*, *Mac1*, *Adam8*, *Mip1α*, and *Tnfα*), and decreased expression of the beneficial adipokine *adiponectin* (Fig. 5*I*) in the abdomen fat. The effect of *Est* ablation on WAT inflammation was absent in *obe* females (Supplementary Fig. 5). These results suggested a potential link between β-cell loss and increased adipose inflammation caused by *Est* ablation in *obe* male mice.

DISCUSSION

In this study, we showed that induction of hepatic *Est* was a phenotype shared by several type 2 diabetes mouse models. The induction of *Est* most likely played a pathogenic role in type 2 diabetes because loss of *Est* in female mice improved metabolic function in *ob/ob*, DEX, and HFD models of type 2 diabetes. The metabolic benefit of *Est* ablation in female *obe* mice seemed attributed to decreased estrogen deprivation and increased estrogenic activity in the liver, underscoring the importance of liver estrogen signaling in protecting females from developing metabolic disease. EST is a GR target gene (11). The pathogenic role of EST in type 2 diabetes is consistent with the observations that *ob/ob* mice had an increased glucocorticoid level, and DEX was sufficient to induce hyperglycemia. It is clear that estrogens and glucocorticoids have beneficial and detrimental effect on insulin sensitivity, respectively. We have shown that glucocorticoids can antagonize estrogenic activity through the regulation of *EST* (11). It is possible that in women, the detrimental effect of glucocorticoids on

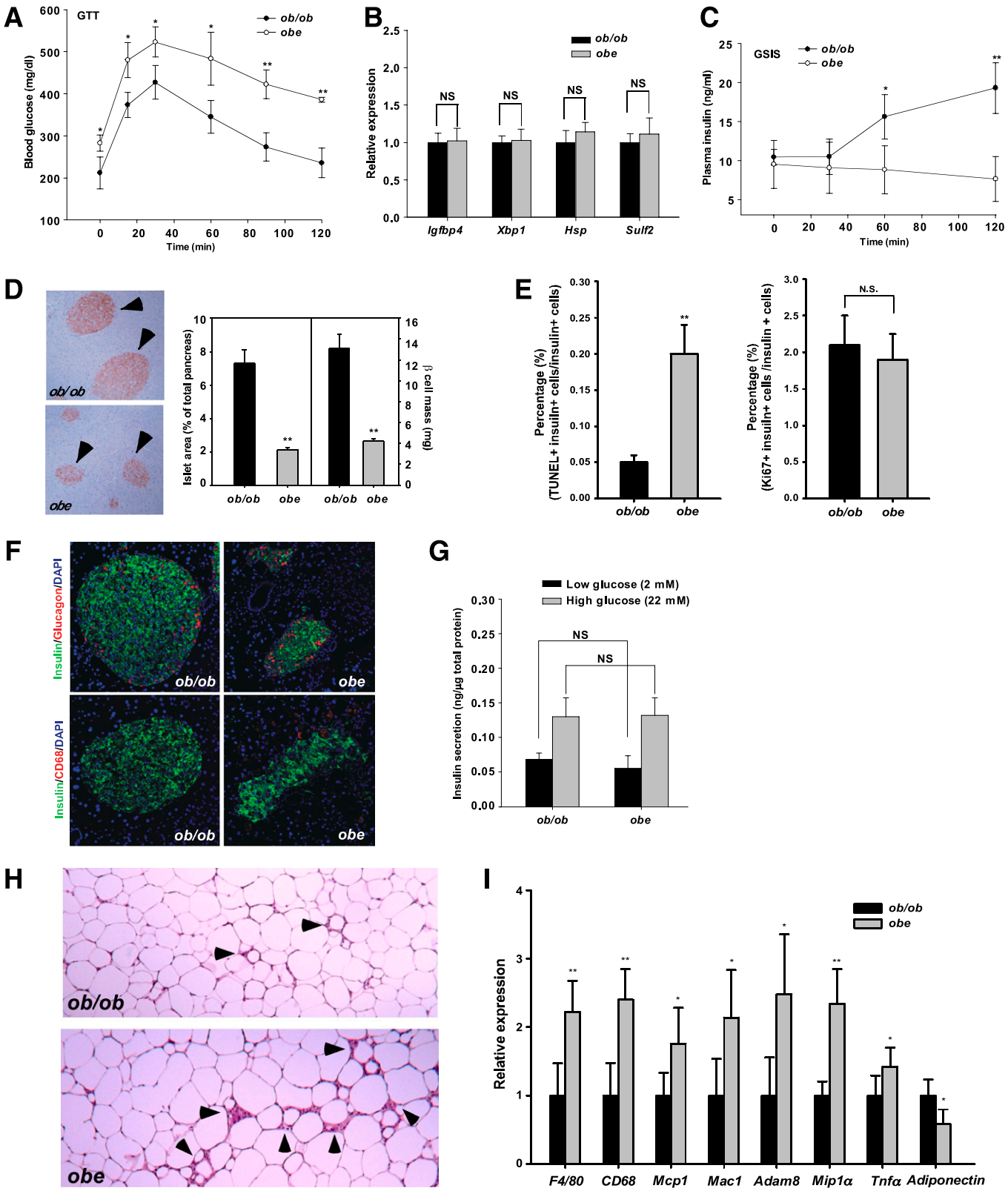

FIG. 5. Loss of *Est* in *ob/ob* male mice aggravated diabetic phenotype, caused a loss of pancreatic β-cell mass, and increased WAT inflammation. *A*: GTT in *ob/ob* and *obe* male mice. *B*: Hepatic expression of estrogen-responsive genes in intact male mice as measured by real-time PCR analysis. *C*: In vivo GSIS test. *D*: Immunostaining of insulin and quantification of total islet area. Arrowheads indicate islets. *E*: β-Cell apoptosis and proliferation were measured by TUNEL assay (*left*) and Ki67 immunostaining (*right*), respectively. In both assays, the sections were counterstained with insulin. *F*: Immunofluorescence analysis of insulin, glucagon, and CD68 expression. *G*: In vitro GSIS test on isolated pancreatic islets. *H*: H-E staining of abdomen adipose tissue. Arrowheads indicate crownlike structures. *I*: Expression of macrophage markers and inflammatory genes as determined by real-time PCR. The expression of each gene was arbitrarily set as 1 in *ob/ob* mice. $N \geq 4$ for each group. *$P < 0.05$; **$P < 0.01$; NS, statistically not significant, *ob/ob* versus *obe*. (A high-quality digital representation of this figure is available in the online issue.)

energy metabolism may become dominant with the onset of menopause because of the major reduction in estrogen production.

Several other lines of anecdotal evidence also suggested that EST may be an important mediator in the pathogenesis of type 2 diabetes in rodents and humans. The expression of *Est* was elevated in the liver of cystic fibrosis transmembrane conductance regulator knockout mice (26). Cystic fibrosis patients are known to have a higher risk of diabetes (27,28). In contrast, several antidiabetic phytoestrogens, such as equol and genistein, have been reported as potent enzymatic inhibitors of EST (29). The causal effect of the expression and/or regulation of EST on the pathogenesis of type 2 diabetes in human patients remain to be confirmed.

It is interesting to note that *Est* deficiency led to increased lean mass and skeletal muscle fiber bundle size, which was associated with an increased expression of liver IGF-1, an important growth-promoting endocrine factor (22). IGF-1 has been implicated in skeletal muscle growth and regeneration, and a viral delivery of the *IGF-1* gene attenuated skeletal muscle atrophy and restored muscle mass and strength in mice (30). The production of IGF-1 is regulated by estrogens. Specifically, activation of ERα was necessary for a systemic production of IGF-1, whereas ablation of ERα in the liver decreased the circulating level of IGF-1 (31). Our data suggested that the relieved muscle hypotrophy in female *obe* mice was likely due to the increased IGF-1 secretion as a result of increased estrogenic activity in the liver.

We were surprised to find that *Est* ablation exacerbated the diabetic phenotype in male *ob/ob* mice. Although sexual dimorphism has been documented in diabetic models, and female mice are in general less susceptible to type 2 diabetes (5,32), previous reports on aromatase and ERα knockout mice suggested that estrogens also exert metabolic benefits in male mice (1,2). The discrepancy may be due to the tissue-specific effect of estrogens. Our *obe* mouse model mainly reflected the hepatic effect of estrogens, because both the induction of *Est* and activation of estrogen-responsive genes in *obe* females were liver-specific. The exacerbated diabetic phenotype in male *obe* mice seemed to be due to compromised insulin secretion. Because the expression of *Est* cannot be detected in the islets, and isolated islets from *ob/ob* and *obe* male mice showed a similar insulin secretion upon glucose stimulation, the lack of insulin secretion in vivo was most likely caused by an insufficient mass of β-cells to maintain glucose homeostasis and driven by factors other than the intrinsic loss of *Est* in β-cells.

Our results suggest that the reduction in β-cell mass in *obe* male mice was mainly caused by increased β-cell death, which was associated with enhanced macrophage infiltration. Because islet phenotypes in *obe* male mice appeared to have been driven by extrapancreatic factors, it is with great interest that we observed increased macrophage infiltration and inflammation, specifically in male WAT (Fig. 5*H* and *I*), given the fact that basal expression of *Est* in WAT follows a sexually dimorphic manner—abundantly expressed in male but barely detectable in female mice (33). It is tempting to speculate that increased inflammation along with decreased synthesis of adiponectin, a beneficial adipokine, in WAT led to low-grade systemic inflammatory response, exaggerated insulin resistance in *obe* male mice, which was followed by failure of β-cell compensation in the late stage. Indeed, we had observed worsened insulin sensitivity in *obe* males at 12 weeks old (Supplementary Fig. 6), the early stage of β-cell compensation in *ob/ob* mice (34). The relationship between *Est* ablation and increased inflammation in male WAT under diabetic condition is another intriguing topic for future investigation. Although estrogens have been reported to suppress lipogenesis and exert anti-inflammatory effects in WAT (35,36), most of the studies were conducted in ovariectomized or ER whole-knockout mice. The direct action of estrogens in adipose tissue, especially regarding its sexually dimorphic manner, to our best knowledge, has not been fully examined. The fact that *Est* is highly expressed in male adipose tissue and $Est^{-/-}$ male displayed larger adipocyte size (33) suggests that estrogen signaling in male WAT may be strictly regulated under normal physiological conditions, and excess estrogens may cause adverse effects, instead of beneficial ones as we expected, to males, especially under extremely obese conditions such as *ob/ob* mice. In fact, several lines of evidence suggested that testosterone has antiobesity effects, and its deprivation in men contributes to the development of metabolic syndrome. We and other groups (37,38) have also reported that overexpression of *Est* in WAT inhibited adipogenesis. The future creation of adipose-specific $Est^{-/-}$ mice will help to understand the direct effect of *Est* and estrogen signaling in male adipose tissue.

In summary, we have uncovered a critical role of *Est* in energy and glucose homeostasis during the pathogenesis of type 2 diabetes. Our results suggested that hepatic estrogen signaling modulated by *Est* induction may represent an important mediator of sex-specific phenotypes usually observed in type 2 diabetes mouse models, even without apparently affecting systemic circulating estrogens. Hepatic *Est*, at least in females, may represent a therapeutic target for the management of type 2 diabetes.

ACKNOWLEDGMENTS

This work was supported in part by National Institutes of Health grants DK-083952 and ES-019629 (to W.X.).

No other potential conflicts of interest relevant to this article were reported.

J.G. designed and performed experiments and wrote the manuscript. J.H., X.S., M.S.-R., and M.X. helped with experiments. R.M.O. and A.G.-O. contributed to the discussion and review of the manuscript. W.X. obtained funding, designed experiments, and wrote the manuscript. J.G. and W.X. are the guarantors of this work and, as such, had full access to all the data in the study and take responsibility for the integrity of the data and the accuracy of the data analysis.

The authors thank Juan Carlos Alvarez-Perez and Rachel Eileen Stamateris from the Division of Endocrinology and Metabolism, University of Pittsburgh, for help with the TUNEL assay and Ki67 immunostaining. The authors also thank Dr. Xin-xin Ding from the Wadsworth Center, New York State Department of Health, and Dr. Jinbo Pi from the Hamner Institute for Health Sciences for helpful comments and suggestions.

REFERENCES

1. Jones ME, Thorburn AW, Britt KL, et al. Aromatase-deficient (ArKO) mice have a phenotype of increased adiposity. Proc Natl Acad Sci U S A 2000;97:12735–12740
2. Heine PA, Taylor JA, Iwamoto GA, Lubahn DB, Cooke PS. Increased adipose tissue in male and female estrogen receptor-alpha knockout mice. Proc Natl Acad Sci USA 2000;97:12729–12734
3. Musatov S, Chen W, Pfaff DW, et al. Silencing of estrogen receptor alpha in the ventromedial nucleus of hypothalamus leads to metabolic syndrome. Proc Natl Acad Sci USA 2007;104:2501–2506

4. Ribas V, Nguyen MT, Henstridge DC, et al. Impaired oxidative metabolism and inflammation are associated with insulin resistance in ERalpha-deficient mice. Am J Physiol Endocrinol Metab 2010;298:E304–E319
5. Riant E, Waget A, Cogo H, Arnal JF, Burcelin R, Gourdy P. Estrogens protect against high-fat diet-induced insulin resistance and glucose intolerance in mice. Endocrinology 2009;150:2109–2117
6. Gao H, Bryzgalova G, Hedman E, et al. Long-term administration of estradiol decreases expression of hepatic lipogenic genes and improves insulin sensitivity in ob/ob mice: a possible mechanism is through direct regulation of signal transducer and activator of transcription 3. Mol Endocrinol 2006;20:1287–1299
7. Hobkirk R. Steroid sulfation Current concepts. Trends Endocrinol Metab 1993;4:69–74
8. Qian YM, Sun XJ, Tong MH, Li XP, Richa J, Song WC. Targeted disruption of the mouse estrogen sulfotransferase gene reveals a role of estrogen metabolism in intracrine and paracrine estrogen regulation. Endocrinology 2001;142:5342–5350
9. Tong MH, Jiang H, Liu P, Lawson JA, Brass LF, Song WC. Spontaneous fetal loss caused by placental thrombosis in estrogen sulfotransferase-deficient mice. Nat Med 2005;11:153–159
10. Gong H, Guo P, Zhai Y, et al. Estrogen deprivation and inhibition of breast cancer growth in vivo through activation of the orphan nuclear receptor liver X receptor. Mol Endocrinol 2007;21:1781–1790
11. Gong H, Jarzynka MJ, Cole TJ, et al. Glucocorticoids antagonize estrogens by glucocorticoid receptor-mediated activation of estrogen sulfotransferase. Cancer Res 2008;68:7386–7393
12. Leiter EH, Chapman HD. Obesity-induced diabetes (diabesity) in C57BL/KsJ mice produces aberrant trans-regulation of sex steroid sulfotransferase genes. J Clin Invest 1994;93:2007–2013
13. Song WC, Moore R, McLachlan JA, Negishi M. Molecular characterization of a testis-specific estrogen sulfotransferase and aberrant liver expression in obese and diabetogenic C57BL/KsJ-db/db mice. Endocrinology 1995;136:2477–2484
14. Leiter EH, Chapman HD, Falany CN. Synergism of obesity genes with hepatic steroid sulfotransferases to mediate diabetes in mice. Diabetes 1991;40:1360–1363
15. Wittmers LE Jr, Haller EW. Effect of adrenalectomy on the metabolism of glucose in obese (C57 Bl/6J ob/ob) mice. Metabolism 1983;32:1093–1100
16. Gill AM, Leiter EH, Powell JG, Chapman HD, Yen TT. Dexamethasone-induced hyperglycemia in obese Avy/a (viable yellow) female mice entails preferential induction of a hepatic estrogen sulfotransferase. Diabetes 1994;43:999–1004
17. Kim JK. Hyperinsulinemic-euglycemic clamp to assess insulin sensitivity in vivo. Methods Mol Biol 2009;560:221–238
18. García-Ocaña A, Vasavada RC, Cebrian A, et al. Transgenic overexpression of hepatocyte growth factor in the beta-cell markedly improves islet function and islet transplant outcomes in mice. Diabetes 2001;50:2752–2762
19. Gao J, He J, Zhai Y, Wada T, Xie W. The constitutive androstane receptor is an anti-obesity nuclear receptor that improves insulin sensitivity. J Biol Chem 2009;284:25984–25992
20. Velazquez-Garcia S, Valle S, Rosa TC, et al. Activation of protein kinase C-ζ in pancreatic β-cells in vivo improves glucose tolerance and induces β-cell expansion via mTOR activation. Diabetes 2011;60:2546–2559
21. Ng KY, Yong J, Chakraborty TR. Estrous cycle in ob/ob and ovariectomized female mice and its relation with estrogen and leptin. Physiol Behav 2010;99:125–130
22. Ohlsson C, Mohan S, Sjögren K, et al. The role of liver-derived insulin-like growth factor-I. Endocr Rev 2009;30:494–535
23. Bartell SM, Rayalam S, Ambati S, et al. Central (ICV) leptin injection increases bone formation, bone mineral density, muscle mass, serum IGF-1, and the expression of osteogenic genes in leptin-deficient ob/ob mice. J Bone Miner Res 2011;26:1710–1720
24. Butler AA, Kozak LP. A recurring problem with the analysis of energy expenditure in genetic models expressing lean and obese phenotypes. Diabetes 2010;59:323–329
25. Kester MH, van Dijk CH, Tibboel D, et al. Sulfation of thyroid hormone by estrogen sulfotransferase. J Clin Endocrinol Metab 1999;84:2577–2580
26. Li L, Falany CN. Elevated hepatic SULT1E1 activity in mouse models of cystic fibrosis alters the regulation of estrogen responsive proteins. J Cyst Fibros 2007;6:23–30
27. Moran A, Pyzdrowski KL, Weinreb J, et al. Insulin sensitivity in cystic fibrosis. Diabetes 1994;43:1020–1026
28. Austin A, Kalhan SC, Orenstein D, Nixon P, Arslanian S. Roles of insulin resistance and beta-cell dysfunction in the pathogenesis of glucose intolerance in cystic fibrosis. J Clin Endocrinol Metab 1994;79:80–85
29. Harris RM, Wood DM, Bottomley L, et al. Phytoestrogens are potent inhibitors of estrogen sulfation: implications for breast cancer risk and treatment. J Clin Endocrinol Metab 2004;89:1779–1787
30. Musarò A, McCullagh KJ, Naya FJ, Olson EN, Rosenthal N. IGF-1 induces skeletal myocyte hypertrophy through calcineurin in association with GATA-2 and NF-ATc1. Nature 1999;400:581–585
31. Della Torre S, Rando G, Meda C, et al. Amino acid-dependent activation of liver estrogen receptor alpha integrates metabolic and reproductive functions via IGF-1. Cell Metab 2011;13:205–214
32. Liu S, Mauvais-Jarvis F. Minireview: Estrogenic protection of beta-cell failure in metabolic diseases. Endocrinology 2010;151:859–864
33. Khor VK, Tong MH, Qian Y, Song WC. Gender-specific expression and mechanism of regulation of estrogen sulfotransferase in adipose tissues of the mouse. Endocrinology 2008;149:5440–5448
34. Coleman DL, Hummel KP. The influence of genetic background on the expression of the obese (Ob) gene in the mouse. Diabetologia 1973;9:287–293
35. Ribas V, Drew BG, Le JA, et al. Myeloid-specific estrogen receptor alpha deficiency impairs metabolic homeostasis and accelerates atherosclerotic lesion development. Proc Natl Acad Sci USA 2011;108:16457–16462
36. Mauvais-Jarvis F. Estrogen and androgen receptors: regulators of fuel homeostasis and emerging targets for diabetes and obesity. Trends Endocrinol Metab 2011;22:24–33
37. Khor VK, Dhir R, Yin X, Ahima RS, Song WC. Estrogen sulfotransferase regulates body fat and glucose homeostasis in female mice. Am J Physiol Endocrinol Metab 2010;299:E657–E664
38. Wada T, Ihunnah CA, Gao J, et al. Estrogen sulfotransferase inhibits adipocyte differentiation. Mol Endocrinol 2011;25:1612–1623